International Scholarly Research Network
ISRN Civil Engineering
Volume 2011, Article ID 282346, 7 pages
doi:10.5402/2011/282346

Research Article

Effectiveness of Information from Vehicles beyond Nearest Vehicle Ahead for Traffic Flow

Hikaru Shimizu, Sho Nishiyama, Yukiko Wakita, and Eisuke Kita

Graduate School of Information Science, Nagoya University, Nagoya 464-8601, Japan

Correspondence should be addressed to Hikaru Shimizu, 2002shimizu@ns.ipl.cs.is.nagoya-u.ac.jp

Received 6 August 2011; Accepted 14 September 2011

Academic Editor: Y. Lai

A driver usually controls the vehicle according to only the information from the nearest leader vehicle. If the information from the other leader vehicles is also available, the driver can control the vehicle more adequately. The aim of this study is to discuss the effectiveness of the information from the other leader vehicles than the nearest one for the traffic flow. For this purpose, the traffic flow is modeled by using the Chandler-type multi-vehicle-following model. This model changes the vehicle acceleration rate according to the velocity differences between the vehicle and its multileader vehicles. After the model stability analysis, the traffic flow simulation is performed. The results reveal that the stable region of the model parameters expands according to the increase of the number of the leader vehicles.

1. Introduction

According to the development of the in-vehicle information technology and the vehicle-to-vehicle communication system, a driver can get the accurate information not only from his nearest leader vehicle but also from the other leader vehicles. If the driver can get such information, he can control his vehicle more adequately and, thus, can avoid the traffic jam. Due to the limitation of the information system, it is difficult to process enormous information in the real time, and thus the available information is restricted fairly.

The aim of this study is to discuss the effect of the information from the far leader vehicles for the traffic flow. If the effect from the far leader vehicles is negligible, the driver can control safely and efficiently his vehicle according to only the information from the near leader vehicles. For this purpose, the traffic flow is modeled by the vehicle-following model [1–9]. Many researchers have presented several vehicle-following models. In Newell model [5], the vehicle acceleration rate is defined as the function of the distance between the vehicle and its nearest leader vehicle. In Chandler model [1], the vehicle acceleration rate depends on the velocity difference between the vehicle and the nearest leader vehicle. In Bierley model [6], the vehicle acceleration rate depends on both the vehicle head distance and the velocity difference between the vehicle and its nearest leader vehicle. In optimal velocity model [7, 10, 11], the acceleration rate is assumed to be proportional to the difference between the vehicle velocity and the optimal velocity function which is defined as the nonlinear function of the distance between the vehicle and its nearest leader vehicle. Chandler-type multi-vehicle-following model is adopted in this study. Chandler-type multi-vehicle-following model, which is a simple extension of the Chandler model, changes the vehicle acceleration rate according to the velocity difference between the vehicle and its multiple leader vehicles.

First, the model stability analysis gives the stable region of the model parameters. The relationship between the stable region and the number of the leader vehicles reveals the effect of the far (or near) leader vehicles for the traffic flow. Next, the traffic flow simulation using the cellular automata model is performed. The cellular automata model is based on the stochastic velocity model [12–14]. In this model, the vehicle movement and velocity are controlled by the help of the uniform random number. In the numerical examples, the effect of the number of the leader vehicles for the traffic flow stabilization is discussed.

The remaining part of this paper is organized as follows. In Section 2, the vehicle-following model and the cellular automata model are explained briefly. The stability analysis of the multi-vehicle-following model and the model dynamics are explained in Sections 3 and 4, respectively. The traffic simulation based on cellular automata model is explained in Section 5. Numerical results are shown in Section 6. Finally, the conclusions are summarized in Section 7.

2. Background

2.1. Vehicle-Following Model. The vehicle-following model is defined so that the vehicle velocity depends on the information from its nearest leader vehicle such as the vehicle distance and the velocity difference.

Newell presents the model that the vehicle acceleration rate depends on the distance between the vehicle and its nearest leader vehicle [5]. Chandler presents the model that the vehicle acceleration rate depends on the velocity difference between the vehicle and the nearest leader vehicle [1].

In Bierley and other models [2–4, 6], the vehicle acceleration rate depends on both the vehicle head distance and the velocity difference between the vehicle and its nearest leader vehicle. Bexelius [8] and Wakita et al. [9] extend the Chandler type model to the multi-leader-following model.

In optimal velocity model [7, 10, 11], the acceleration rate is assumed to be proportional to the difference between the vehicle velocity and the optimal velocity function which is defined as the nonlinear function of the distance between the vehicle and its nearest leader vehicle.

2.2. Cellular Automata Model. The first traffic simulation model based on cellular automata was presented by Wolfram as the rule-184 CA model [15]. In this model, the vehicles do not accelerate even when the leader vehicle is very far. Therefore, the rule-184 CA model cannot simulate the actual traffic flows well.

The Nagel-Schreckenberg (NaSch) model is composed of the rule-184 CA model and the rules for acceleration and deceleration of vehicles [16]. The vehicle velocity is represented according to the number of cells which a vehicle moves over at each time step. When it is applied to urban city traffic flow, the behavior rules of the vehicles become very complicated due to the existence of the traffic signals, the intersections, and the branch lines.

Authors have presented the stochastic velocity (SV) model [12–14, 17]. In this model, a vehicle velocity v is represented with the stochastic variable P as follows:

$$v = v_{\max} \times P, \tag{1}$$

where P denotes the stochastic variable from 0 to 1 and $v_{\max}$ is the maximum velocity of the vehicle.

In this model, the vehicles driving at velocity of $v_{\max}$ can move by one cell at each time step. The movement of the vehicles at velocity of $v(< v_{\max})$ is determined according to the stochastic variable P. Since the maximum movable distance of vehicles is restricted up to one cell, the vehicle behavior rules can be simplified.

3. Model Stability Analysis

3.1. Muti-Vehicle-Following Model. Chandler-type multi-vehicle-following model is defined as

$$\ddot{x}_n(t+\Delta t) = \sum_{j=1}^{m} a_j \left(\dot{x}_{n-j}(t) - \dot{x}_n(t)\right), \tag{2}$$

where $x_n(t) > 0$ is the nth vehicle position, $a_j > 0$ is driver's sensitivity to the jth leader vehicle for the nth vehicle, and $\Delta t > 0$ is the delay time. The upper dot denotes the differentiation with respect to the time. The value m is the number of the leader vehicles. In this model, the vehicle acceleration rate $\ddot{x}_n$ is controlled according to the velocity difference $\dot{x}_{n-j}(t) - \dot{x}_n(t)$.

Since the sensitivity with respect to the near leader vehicle is stronger than that with respect to the farer ones, the following relationship exists between the sensitivities:

$$a_1 \geq a_2 \geq \cdots \geq a_m. \tag{3}$$

3.2. Stability Analysis. In (2), we will consider the stable state that all vehicles move at the same velocity v_0.

Let y_n be a small deviation from the steady state velocity;

$$\dot{x}_n = v_0 + y_n. \tag{4}$$

Substituting (4) to (2), we have

$$\dot{y}_n(t+\Delta t) = \sum_{j=1}^{m} a_j \left(y_{n-j}(t) - y_n(t)\right). \tag{5}$$

The following equations are regarded as Fourier series of y_n

$$\begin{gathered} y_k(n,t) = \exp(i\alpha_k n + zt), \\ \alpha_k = \frac{2\pi}{N}k, \quad k = 0, 1, 2, \ldots, N-1, \end{gathered} \tag{6}$$

where N and i denote total number of vehicles and the imaginary unit, respectively. Besides, $z = u + iv$ (u and v are real) satisfies

$$e^{\Delta t z} z - \sum_{j=1}^{m} a_j \left(e^{ji\alpha_k} - 1\right) = 0. \tag{7}$$

Applying Taylor series expansion ($e^{\Delta t z} \cong 1 + \Delta t z$) to (7), we have

$$\Delta t z^2 + z - \sum_{j=1}^{m} a_j \left(e^{ji\alpha_k} - 1\right) = 0. \tag{8}$$

If the real part of z in (8) is positive ($u > 0$), (6) shows that y_k diverges as the time develops, and therefore, the solution of (2) becomes unstable. If the real part of z is negative ($u < 0$), the solution of (6) shows that y_k converges to zero as the time develops and therefore, the solution of (2) becomes stable. If the real part of z is zero ($u = 0$), the solution of (2) oscillates.

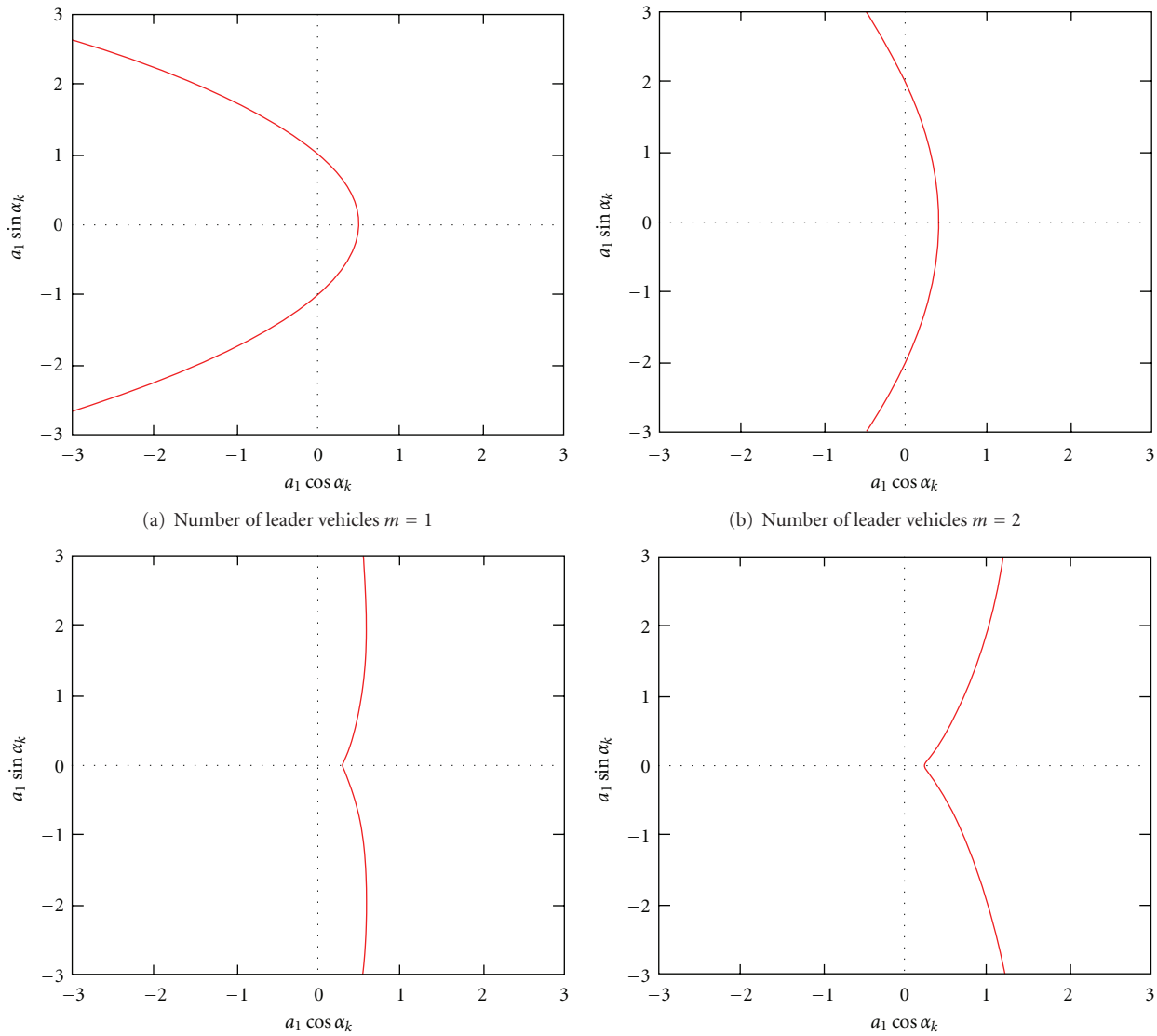

(a) Number of leader vehicles $m = 1$

(b) Number of leader vehicles $m = 2$

(c) Number of leader vehicles $m = 3$

(d) Number of leader vehicles $m = 4$

Figure 1: Limit curves.

4. Model Dynamics

At a critical point, $u = 0$. Therefore, z becomes a pure imaginary number. Substituting $z = ip$ to (8), we have

$$(-\Delta t p^2 + \sigma_c) + i(p - \sigma_s) = 0, \tag{9}$$

where

$$\sigma_c = \sum_{j=1}^{m} a_j \{1 - \cos(\alpha_k j)\},$$
$$\sigma_s = \sum_{j=1}^{m} a_j \sin(\alpha_k j). \tag{10}$$

From (9), we have the following simultaneous equations:

$$-\Delta t p^2 + \sigma_c = 0,$$
$$p - \sigma_s = 0. \tag{11}$$

Deleting p from (11), we have

$$\Delta t = \frac{\sigma_c}{\sigma_s^2}. \tag{12}$$

4.1. Case $m = 1$. Substituting $m = 1$ to (12), we have

$$a_1 = \frac{1}{2\Delta t \cos^2(\alpha_k/2)}. \tag{13}$$

Taking the delay time $\Delta t = 1$, we have

$$a_1 = \frac{1}{2\cos^2(\alpha_k/2)}. \tag{14}$$

Substituting $\alpha_k = 0$ to (13), we have the following stability condition:

$$a_1 < \frac{1}{2\Delta t}. \tag{15}$$

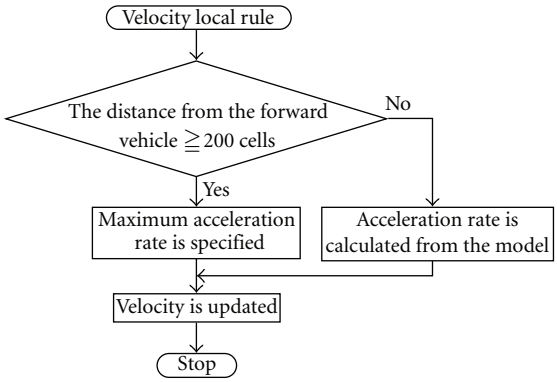

Figure 2: Velocity local rule.

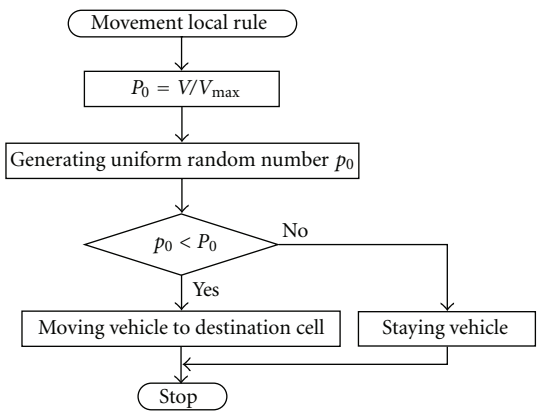

Figure 3: Movement local rule.

4.2. Case $m = 2$. Substituting $m = 2$ to (12), we have

$$\Delta t = \frac{a_1 + 2a_2(1+\cos\alpha_k)}{2(a_1 + 2a_2\cos\alpha_k)^2\cos^2(\alpha_k/2)}. \tag{16}$$

Substituting $\alpha_k = 0$ to the above equation, we have the stability condition

$$\frac{(a_1 + 2a_2)^2}{a_1 + 4a_2} < \frac{1}{2\Delta t}. \tag{17}$$

Taking $\Delta t = 1$ and assuming $a_2/a_1 = 1/2$ in (16), we have

$$a_1 = \frac{2 + \cos\alpha_k}{2(1+\cos\alpha_k)^2\cos^2(\alpha_k/2)}. \tag{18}$$

4.3. Case $m = 3$. Substituting $m = 3$ to (12), we have

$$\Delta t = \frac{a_1 + 2a_2(1+\cos\alpha_k) + a_3\left(4\cos^2\alpha_k + 4\cos\alpha_k + 1\right)}{2(a_1 + 2a_2\cos\alpha_k + a_3(4\cos^2\alpha_k - 1))^2\cos^2(\alpha_k/2)}. \tag{19}$$

Substituting $\alpha_k = 0$ to the above equation, we have the stability condition as follows:

$$\frac{(a_1 + 2a_2 + 3a_3)^2}{a_1 + 4a_2 + 9a_3} < \frac{1}{2\Delta t}. \tag{20}$$

Taking $\Delta t = 1$ and assuming $a_2/a_1 = 2/3$ and $a_3/a_1 = 1/3$ in (20), we have

$$a_1 = \frac{1 + (4/3)(1+\cos\alpha_k) + (1/3)\left(4\cos^2\alpha_k + 4\cos\alpha_k + 1\right)}{2(1 + (4/3)\cos\alpha_k + (1/3)(4\cos^2\alpha_k - 1))^2\cos^2(\alpha_k/2)}. \tag{21}$$

4.4. Case $m = 4$. Substituting $m = 4$ to (12), we have

$$\Delta t = \frac{a_1 + 2a_2(1+\cos\alpha_k) + a_3\left(4\cos^2\alpha_k + 4\cos\alpha_k + 1\right) + 4a_4(1+\cos\alpha_k)(1+\cos 2\alpha_k)}{2\{a_1 + 2a_2\cos\alpha_k + a_3(4\cos^2\alpha_k - 1) + 4a_4\cos\alpha_k\cos 2\alpha_k\}^2\cos^2(\alpha_k/2)}. \tag{22}$$

Substituting $\alpha_k = 0$ to the above equation, we have the stability condition as follows:

$$\frac{(a_1 + 2a_2 + 3a_3 + 4a_4)^2}{a_1 + 4a_2 + 9a_3 + 16a_4} < \frac{1}{2\Delta t}. \tag{23}$$

Taking $\Delta t = 1$ and assuming $a_2/a_1 = 3/4$, $a_3/a_1 = 2/4$, and $a_4/a_1 = 1/4$ in (23), we have

$$a_1 = \frac{1 + (3/2)(1+\cos\alpha_k) + (1/2)\left(4\cos^2\alpha_k + 4\cos\alpha_k + 1\right) + (1+\cos\alpha_k)(1+\cos 2\alpha_k)}{2\{1 + (3/2)\cos\alpha_k + (1/2)(4\cos^2\alpha_k - 1) + \cos\alpha_k\cos 2\alpha_k\}^2\cos^2(\alpha_k/2)}. \tag{24}$$

4.5. Discussion. The upper limits of the sensitivities at $m = 1$, 2, 3, and 4 are given by (14), (18), (21), and (24), respectively. The limit curves are shown in Figures 1(a), 1(b), 1(c), and 1(d). We notice from the figures that the stable zone is

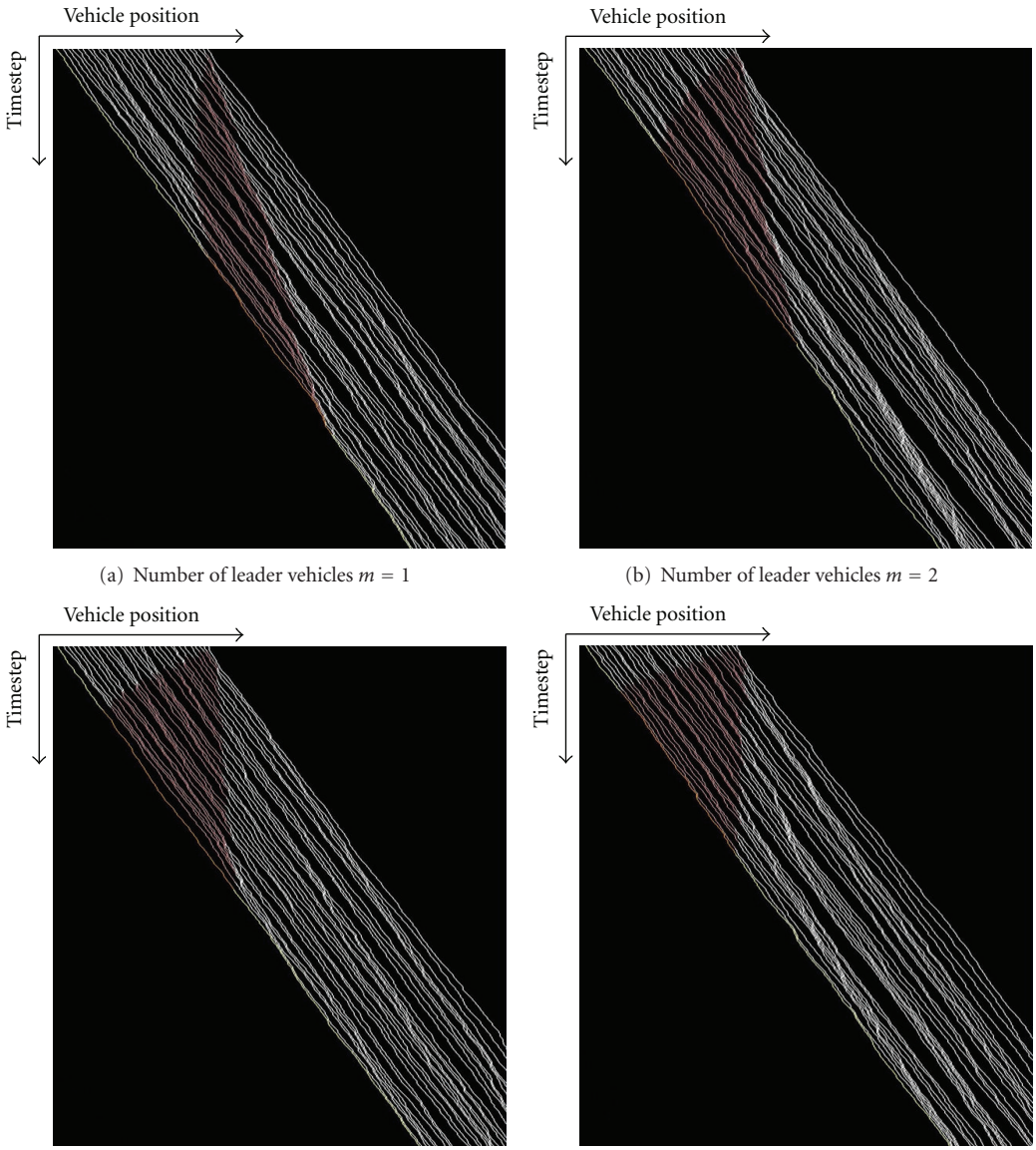

(a) Number of leader vehicles $m = 1$

(b) Number of leader vehicles $m = 2$

(c) Number of leader vehicles $m = 3$

(d) Number of leader vehicles $m = 4$

Figure 4: Traffic flow.

growing as the number of the leader vehicles m increases. In case of wider stable zone, the lager sensitivities are available, and thus, vehicles can change their velocity more quickly. Therefore, it is concluded that the traffic flow is more stable as the number of the leader vehicles increases.

5. Cellular Automata Model

5.1. Object Domain. In cellular automata simulation, the object domain is represented with square cells with 3(m) width and 3(m) length. One vehicle is indicated with two cells and therefore, it has 3(m) width and 6(m) length.

5.2. Simulation Process. Simulation process can be summarized as follows. The parameter t denotes the simulation time step and one simulation time step denotes 0.1(s) in real-time.

(1) The time step t is initialized.

(2) Vehicles are distributed in the object domain.

(3) Vehicle distances from all vehicles to the other vehicles ahead are estimated.

(4) Velocity local rule is applied to all vehicles.

(5) Movement local rule is applied to all vehicles.

(6) $t \leftarrow t + 1$.

(7) The process goes to step (2).

5.3. Local Rule

5.3.1. Vehicle Distance. The vehicle distance G is defined as the distance from the vehicle to the nearest leader vehicle.

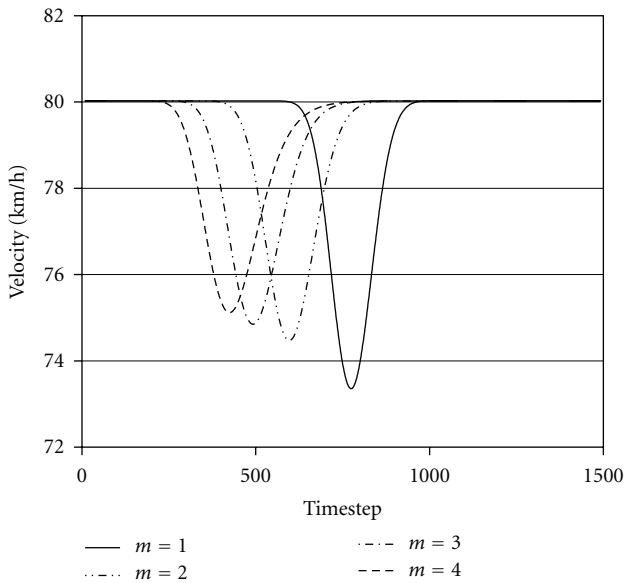

Figure 5: Rearmost vehicle velocity.

5.3.2. Velocity Local Rule. The vehicle velocity is changed according to the velocity local rule. The velocity local rule algorithm is illustrated in Figure 2.

(1) If $G \geq 200$ cells (600 m), the vehicle acceleration rate is specified to the maximum value 2.4 (m/sec^2), which is determined from the actual traffic data [12].

(2) If $G < 200$ cells, the vehicle acceleration rate is calculated from (2).

(3) The vehicle velocity is updated by

$$\dot{x}_n(t) = \dot{x}_n(t-1) + \ddot{x}_n \times T, \tag{25}$$

where T denotes the real time for one time step and $T = 0.1$(s).

5.3.3. Movement Local Rule. In this study, vehicles move according to the stochastic velocity model presented by Tamaki et al. [12–14, 17]. In the stochastic velocity model, the vehicle movement is controlled by the help of the uniform random number. The algorithm of the model is illustrated in Figure 3.

(1) The threshold

$$P_0 = \frac{V}{V_{\max}} \tag{26}$$

is calculated from each vehicle velocity V and the maximum velocity $V_{\max}$. The maximum velocity $V_{\max}$ is specified for all vehicles in the object domain.

(2) A uniform random number p_0 is generated within $[0, 1]$.

(3) If $p_0 < P_0$, the vehicle moves by one cell. If not so, the vehicle stays at the cell at this time step.

A vehicle move at most by one cell at each time step.

Table 1: Sensitivities with respect to vehicles ahead.

$m = 1$	$a_1 = 0.40$
$m = 2$	$a_1 = 0.26667$, $a_2 = 0.13333$
$m = 3$	$a_1 = 0.20$, $a_2 = 0.13333$, $a_3 = 0.06667$
$m = 4$	$a_1 = 0.16$, $a_2 = 0.12$, $a_3 = 0.08$, $a_4 = 0.04$

6. Numerical Example

A traffic flow on a one-way road is simulated in the cellular automata model. Maximum velocity is identical in all vehicles and set to 80(km/h). The initial velocity is specified as 40(km/h) for a leader vehicle and 80(km/h) for others, respectively. The delay time is taken as $\Delta t = 1$. Driver's sensitivities are shown in Table 1. The sensitivities are specified so as to satisfy the following conditions described in Section 4:

$$\begin{aligned}
&\sum_{i=1}^{m} a_i = 0.40 \quad (m = 1, 2, 3, 4),\\
&\frac{a_2}{a_1} = \frac{1}{2} \quad (m = 2),\\
&\frac{a_2}{a_1} = \frac{2}{3}, \qquad \frac{a_3}{a_1} = \frac{1}{3} \quad (m = 3),\\
&\frac{a_2}{a_1} = \frac{3}{4}, \qquad \frac{a_3}{a_1} = \frac{2}{4}, \qquad \frac{a_4}{a_1} = \frac{1}{4} \quad (m = 4).
\end{aligned} \tag{27}$$

The traffic flow is shown in Figure 4. The figures are plotted with the vehicle position as the horizontal axis and the time step as the vertical axis, respectively. White curves denote the vehicle trajectories. Figures show that the vehicles change their velocity more quickly as the number of the leader vehicles m increases.

Figure 5 shows the velocity variation of the rearmost vehicle. The figures are plotted with the time step as a horizontal axis and the velocity as the vertical axis, respectively. The maximum velocity reduction is 7, 5.5, 5.0, and 4.5 km/h in case of $m = 1$, 2, 3, and 4, respectively. Therefore, the maximum velocity reduction is smaller with respect to the increase of the parameter m.

7. Conclusion

A driver usually controls the vehicle according to the information from only the nearest leader vehicle. If the information from the other leader vehicles than the nearest one is available, the driver can control his vehicle more adequately. In this study, cellular automata simulation using the Chandler-type multi-vehicle-following model was performed in order to discuss the effectiveness of the information from the other leader vehicles than the nearest one for the traffic flow.

Firstly, the stability analysis of the models revealed that the traffic flow became more stable according to the number of the leader vehicles.

Next, the model parameters were determined and then applied for the cellular automata-based traffic flow simulation. The results showed that, according to the increase of the number of the leader vehicles, the velocity reduction was saved and the velocity recovery time was shortened.

References

[1] R. E. Chandler, R. Herman, and E. W. Montroll, "Traffic dynamics; studies in car-following," *Operations Research*, vol. 6, no. 2, pp. 165–184, 1958.

[2] D. C. Gazis, R. Herman, and R. B. Potts, "Car following theory of steady state traffic flow," *Operations Research*, vol. 7, pp. 499–505, 1959.

[3] L. C. Edie, "Car-following and steady-state theory for noncongested traffic," *Operations Research*, vol. 9, pp. 66–76, 1961.

[4] R. Herman and R. Rothery, "Microscopic and macroscopic aspects of single lane traffic flow," *Operations Research*, vol. 6, pp. 74–93, 1962.

[5] G. F. Newell, "Nonlinear effects in the dynamics of car following," *Operations Research*, vol. 9, no. 2, pp. 209–229, 1961.

[6] R. L. Bierley, "Investigation of an intervehicle spacing display," *Highway Research Record*, vol. 25, pp. 58–75, 1963.

[7] M. Bando, K. Hasebe, K. Nakanishi, A. Nakayama, A. Shibata, and Y. Sugiyama, "Phenomenological study of dynamical model of traffic flow," *Journal of Physics I France*, vol. 5, pp. 1389–1399, 1995.

[8] S. Bexelius, "An extended model for car-following," *Transportation Research*, vol. 2, no. 1, pp. 13–21, 1968.

[9] Y. Wakita, T. Iguchi, H. Shimizu, T. Tamaki, and E. Kita, "Comparison of zipper and non-zipper merging patterns near merging point of roads," *International Journal of Natural Computing Research*, vol. 1, no. 3, pp. 19–29, 2010.

[10] S. Yukawa and M. Kikuchi, "Coupled-map modeling of one-dimensional traffic flow," *Journal of the Physical Society of Japan*, vol. 64, no. 1, pp. 35–38, 1995.

[11] Y. Sugiyama, "Optimal velocity model for traffic flow," *Computer Physics Communications*, vol. 121, pp. 399–401, 1999.

[12] T. Tamaki, S. Yasue, and E. Kita, "Traffic flow simulation using cellular automata," in *Proceedings of Civil and Structural Engineering Computing*, Civil-Comp Press, 2003.

[13] T. Tamaki and E. Kita, "Urban city traffic simulation based on stochastic velocity model," in *Proceedings of the 10th International Conference on Civil, Structural and Environmental Engineering Computing*, pp. 215–216, Civil-Comp Press, 2005.

[14] Y. Wakita, T. Iguchi, H. Shimizu, T. Tamaki, and E. Kita, "Cellular automata simulation of traffic jams at the merging point of roads," in *Proceedings of the 1st International Conference on Soft Computing Technology in Civil, Structural and Environmental Engineering*, B. H. V. Topping and Y. Tsompanakis, Eds., Stirlingshire, UK, 2009.

[15] S. Wolfram, *Cellular Automata and Complexity*, Adison-Wesley, 1st edition, 1994.

[16] K. Nagel and M. Schreckenberg, "Cellular automaton model for freeway traffic," *Journal of Physics I France*, vol. 2, pp. 2221–2229, 1992.

[17] T. Tamaki, S. Yasue, and E. Kita, "City traffic simulation using cellular automata with stochastic velocity model," in *Proceedings of the International Conference on Parallel and Distributed Processing Techniques and Applications (PDPTA '04)*, vol. 12, pp. 440–441, 2004.